Asymmetry in histone rotation in forced unwrapping and force quench rewrapping in a nucleosome

Govardhan Reddy [1,*] **and D. Thirumalai** [2,*]

[1]Solid State and Structural Chemistry Unit, Indian Institute of Science, Bengaluru 560012, Karnataka, India and
[2]Department of Chemistry, The University of Texas, Austin, TX 78712, USA

ABSTRACT

Single molecule pulling experiments have shown that DNA in the nucleosomes unwraps in two stages from the histone protein core (HPC). The first stage, attributed to the rupture of the outer DNA turn, occurs between 3 and 5 pNs, and is reversible. The inner DNA turn ruptures irreversibly at forces between 9 and 15 pNs (or higher) in the second stage. Molecular simulations using the Self-Organized Polymer model capture the experimental findings. The unwrapping of the outer DNA turn is independent of the pulling direction. The rupture of the DNA inner turn depends on the pulling direction and involves overcoming substantial energetic (most likely electrostatic in origin) and kinetic barriers. They arise because the mechanical force has to generate sufficient torque to rotate the HPC by 180°. On the other hand, during the rewrapping process, HPC rotation is stochastic, with force playing no role. The assembly of the outer DNA wrap upon force quench nearly coincides with the unwrapping process, confirming the reversibility of the outer turn rupture. The asymmetry in HPC rotation during unwrapping and rewrapping explains the observed hysteresis in the stretch-release cycles in experiments. We propose experiments to test the prediction that HPC rotation produces kinetic barriers in the unwrapping process.

INTRODUCTION

Genomes in eukaryotes, spanning roughly a meter long when stretched, are efficiently packed in a few micrometer sized cells. This spectacular process occurs routinely, resulting in the compaction of the genome accompanied by a density increase of over six orders of magnitude. The condensed material is chromatin,—a polymer whose building block is the nucleosome (1), made up of a complex between DNA and the highly conserved histone proteins. The $\approx$147 bp, roughly the persistence length of DNA, are wrapped around the ($\approx$10 nm) octameric histone protein core (HPC) (Figure 1). It follows that DNA is tightly wound around the histones $\approx$1.6–1.7 times (Figure 1). Key cellular processes, such as replication, recombination and transcription depend in part on the positioning and the dynamics of the nucleosomes (2,3). Because the primary function of nucleosomes is the regulation of transcription (4), it is important to understand the forces that govern the stability of the nucleosome, and the mechanism by which DNA unwraps and rewraps.

Single molecule pulling experiments on chromatin fibers (5–11), and arrays of nucleosomes and a single nucleosome (5,12–16) have given quantitative insights into their nanomechanics. Of particular relevance here are the pulling experiments on single nucleosomes using the Widom 601 sequence (12), which established that the fully wrapped DNA unravels in two major stages upon application of mechanical force, f (Figure 1). In the first stage, occurring at low forces, $f \approx$ 3–5 pN, the outer turn of the DNA 'rips' or unwraps releasing $\approx 21 \pm 0.22$ nm (roughly 60–70 bp) length of DNA (12–14). In the force range ($f \leq$ 5 pN), DNA hops between the fully wrapped and partially unwrapped states. Thus, it is surmised that the observed two-state hopping is an equilibrium reversible process (12,14). The low force transition is interpreted as peeling of the outer turn in which $\sim$1.6–1.0 turn of DNA is unwound (Figure 1B to C). The second unwrapping stage, which occurs in the force range $f \approx$ 9–15 pN or more $\approx$15–20 pN, is attributed to an irreversible peeling of the inner turn of the DNA (12,14). During this transition there is an additional release of $\approx 22 \pm 0.18$ nm of DNA, which results in unwinding from 1.0 to <0.5 turn (Figure 1C to D). The DNA release during this stage is abrupt (5), and shows signs of hysteresis, inferred from the finding that the force extension curves (FECs) during the stretching/release of force do not coincide (12). We refer to the three dominant states of the wrapped DNA as 1.6**N**, 1.0**N** and 0.5**N**, where **N** stands for nucleosome and the number in front is the amount of DNA turns around the HPC. The numerical values specifying the number of turns are approximate.
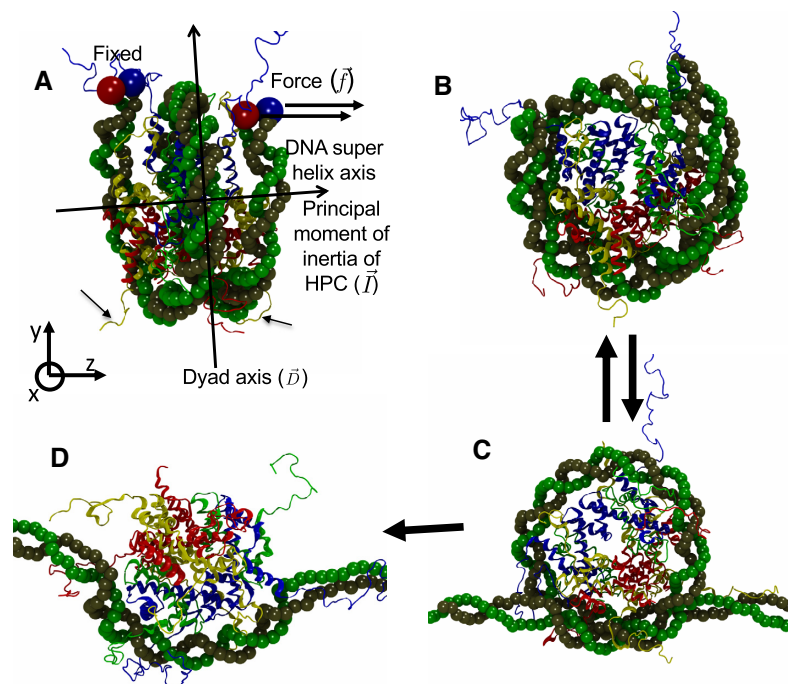
Figure 1. A nucleosome has a double stranded DNA, which wraps around the HPC. DNA strands are shown in tan and green color. Two copies each of the four proteins H2A, H2B, H3 and H4 form the HPC. H2A, H2B, H3 and H4 are colored in yellow, red, blue and green, respectively. (**A**) Nucleosome orientation at the start of the simulations. The two fold nucleosome dyad axis, $\vec{D}$, passing through the center of the wrapped DNA, is along the y direction and lies in the xy plane. The xy plane, through the center of the figure and perpendicular to the plane of the paper roughly separates one copy of the H2A, H2B, H3 and H4 protein complex from the second. The DNA super helix axis and the principal moment of inertia $\vec{I}$ of the HPC point along the z direction and are in the xz plane. The two ends of the double stranded DNA are shown as red and blue beads. One end of the DNA is fixed and a constant force is applied to the other end, either along the x or the z direction. The small slanted arrows point to the histone protein tails, which interact with the DNA. When force is applied to the ends of the DNA, the first reversible structural transition occurs shown as (**B**) to (**C**). The outer DNA turn unwraps from the HPC. The second abrupt irreversible structural transition occurs between (**C**) and (**D**), where the inner turn unwraps. The figure is rendered using Visual Molecular Dynamics (VMD) ([17](#)).

High forces required to peel the inner wrap is larger than estimates using equilibrium arguments (12,18,19). To explain this behavior, it was conjectured that there could be electrostatic attraction between DNA (negatively charged) and the positively charged HPC (5,12). However, neither the crystal structures (20,21) nor the equilibrium accessibility of the nucleosomal DNA provides evidence for such a patch that may be conducive to large favorable interactions between the histones and the partially wrapped DNA (22). This observation prompted Kulic and Schiessel (KS) (22), in a remarkable paper, to propose an alternative explanation. DNA is negatively charged and when the DNA is fully wrapped around the nucleosome, there could be considerable electrostatic repulsion between the inner and outer wraps of the DNA. This unfavorable interaction results in a small free energy barrier observed during the first stage of DNA unraveling. After the first stage of unraveling, the nucleosome transitions to the 1.0N state. Consequently, the unfavorable DNA–DNA electrostatic repulsion is muted, and the structure of the nucleosome is stabilized, which results in a much higher free energy barrier (and hence larger values of f) for unraveling the inner wrap of the DNA. These generic arguments suggest that the global unwrapping mechanism may not be sensitive to the DNA sequence. We hasten to point out that not all nucleosomes are physically identical. The post translational modifications chemically alter the histones. In addition, DNA nanomechanics and dynamics are sequence dependent (23–25).

Given the importance of HPC in the genome organization, it is not surprising that there are many theoretical and computational studies (18,19,22,26–34) probing the stability of nucleosomes. In some of these studies the DNA is modeled as a semi-flexible polymer, and the HPC as a rigid spherical bead or a helical spool (22,30). Such a description is remarkably successful in predicting the two major stages of DNA unwrapping. However, they are not entirely successful in fully explaining the equilibrium nature of the first stage of unwrapping and the kinetically controlled (manifested as hysteresis in the rewrapping of DNA from the 0.5N state upon force quench) second transition. Some of the reasons could be that the theoretical studies assume thermodynamic equilibrium during nucleosome DNA pulling, where as the energy barriers could exist for kinetic reasons. In addition to the theories based on DNA elasticity, coarse-grained simulations have been used to explore the free energy landscape of nucleosomes (32,33). In a study that is related to our investigation (33) force-dependent free energy profile of the DNA as a function of the extension was used to provide quantitative estimates of the unwrapping forces.

Most, if not all, of the computational studies are DNA centric with scant attention to the role that HPC plays in the unwrapping or rewrapping processes. In order to remedy

this situation, we investigate forced-unwrapping and force-quench rewrapping of a single nucleosome using a coarse grained (CG) model of the nucleosome and Brownian dynamics simulations. In accord with experiments, we find that there is a reversible transition from 1.6**N** to 1.0**N** states followed by a transition to the 0.5**N** state at high forces. Upon force quench, we find that there is hysteresis in the 0.5**N** → 1.6**N** transition. We show that hysteresis observed in the pulling experiments is due to the distinctly asymmetric role the external mechanical force plays in the DNA unwrapping and rewrapping pathways. In the second irreversible transition (1.0**N** → 0.5**N**), kinetic barriers arise because sufficient torque has to be generated by the mechanical force to rotate the HPC by nearly 180°. This is resisted by the solvent friction, and the favorable electrostatic interactions between the histone tails and DNA (34). In contrast, rewrapping of the DNA onto the HPC during the second transition upon quenching the force to low values (≤3 pN), occurs only when the principal moment of inertia of the HPC aligns along the pulling direction. The alignment occurs stochastically by thermal fluctuations. The external force does not play a role in aligning the HPC and the DNA. This asymmetry in the role played by HPC rotation dramatically alters the rewrapping pathways, thus contributing to the observed hysteresis in single molecule pulling experiments. We show that the requirement for HPC rotation to unwrap the DNA increases the barrier has both an energetic and a kinematic effect. The latter renders the rupture of the inner turn irreversible. We predict that the time scale to unwrap the inner turn should increase exponentially with the solvent viscosity, which is amenable to experimental test.

MATERIALS AND METHODS

SOP model for the nucleosome

The simulations use the Self-Organized Polymer (SOP) model (35), which has proved to be accurate in describing the dynamics of polymerase-induced transcription bubble formation (36), folding of large proteins (37), effect of force on RNA (35), and cation-dependent folding of a number of RNA molecules (38). Each residue in the histone is represented using a single bead. Following our earlier work (36), we represent the nucleotides in the DNA using a single bead, which is sufficient to characterize the mechanical properties (e.g. persistence length (l_p) and salt-dependent changes in l_p) of DNA accurately. Predictions using the model (36) for bubble formation in promoter DNA during bacterial transcription have found experimental support (39,40), thus validating the model.

In the SOP model, the center of a bead representing the protein residue is at the C_α atom, and the bead representing the nucleotide is at its center of mass. The total energy of the nucleosome is a sum of bonded and non-bonded interactions. The bonds between two neighboring beads in a protein or the DNA sequence are modeled using a finite extensible nonlinear elastic (FENE) potential. The non-bonded interactions are a sum of native and non-native interactions. Interaction between two beads (separated by at least two other beads along the same protein or the DNA sequence) is considered to be native if the distance between them is less than a cutoff value in the coarse grained representation of

the nucleosome crystal structure. The native interactions are modeled using a Lennard-Jones like potential and the non-native interactions are purely repulsive. The interaction between charged beads is modeled using a screened Coulomb potential.

The parameters for the SOP forcefield are given in the Supplementary Information (SI) (Supplementary Table S1). The SOP model for the nucleosome is constructed using the crystal structure (20) of the human nucleosome available in the Protein Data Bank (PDB ID: 2CV5). The 147 bp palindromic DNA sequence from the human α-satellite DNA (21) binds symmetrically to the HPC. The DNA is split into two halves containing 73 and 72 bp, with a single base pair located on the dyad. We performed Brownian dynamics simulations (41) at temperature, $T = 300$ K to determine the mechanism of force-induced unwrapping and force-quench rewrapping of DNA from the nucleosome. Details of the model and the simulation methodology are given in the SI.

RESULTS

Most of the results are obtained without the histone tails, whose role is examined to ensure that the overall unwrapping mechanism is unaltered. In the KS study (22) and subsequent generalizations, it was shown that many (but not all) aspects of tension-induced unwrapping of the nucleosome could be explained using a purely elastic model of the wrapped DNA. To go beyond the elastic model description of DNA and rigid body cylinder representation of the HPC, we use the SOP model for the DNA–protein complex to elucidate the molecular details of DNA unbinding dynamics from the nucleosome with focus on the HPC dynamics on application of constant force.

DNA unwraps in two stages

The orientation of the nucleosome at the start of the simulation is shown in Figure 1A. The principal moment of inertia of the HPC (see SI), $\vec{I}$, is oriented along the z direction. In this orientation, the end-to-end vector of the DNA, $\vec{R}_{ee}$, points along the x direction (Figure 1A). One end of the double stranded DNA is fixed, and a constant force, $\vec{f}$, is applied to the other end on the two beads of the double stranded DNA. When the applied $\vec{f}$ is parallel to $\vec{R}_{ee}$ (along the x direction), it is readily transmitted to the rest of the DNA.

In accord with the experiments and previous simulations using a different coarse-grained model (33,34), we find that DNA unwraps in two stages (12) (Figure 2). It can be concluded that the reversible unwrapping of the outer turn followed by a non-equilibrium rupture of the inner turn, representing the global two stage rupture of DNA, are likely to be independent of the DNA sequence because two different sequences yield the same pattern of DNA rupture. In all the trajectories, the 1.0**N** state is observed as long as the force is applied along the x direction (parallel to $\vec{R}_{ee}$), implying that it is an essential intermediate in the forced-rupture of the nucleosome. Pulling experiments (12) find that a transition from 1.6**N** turns to 1.0**N** turn occurs in
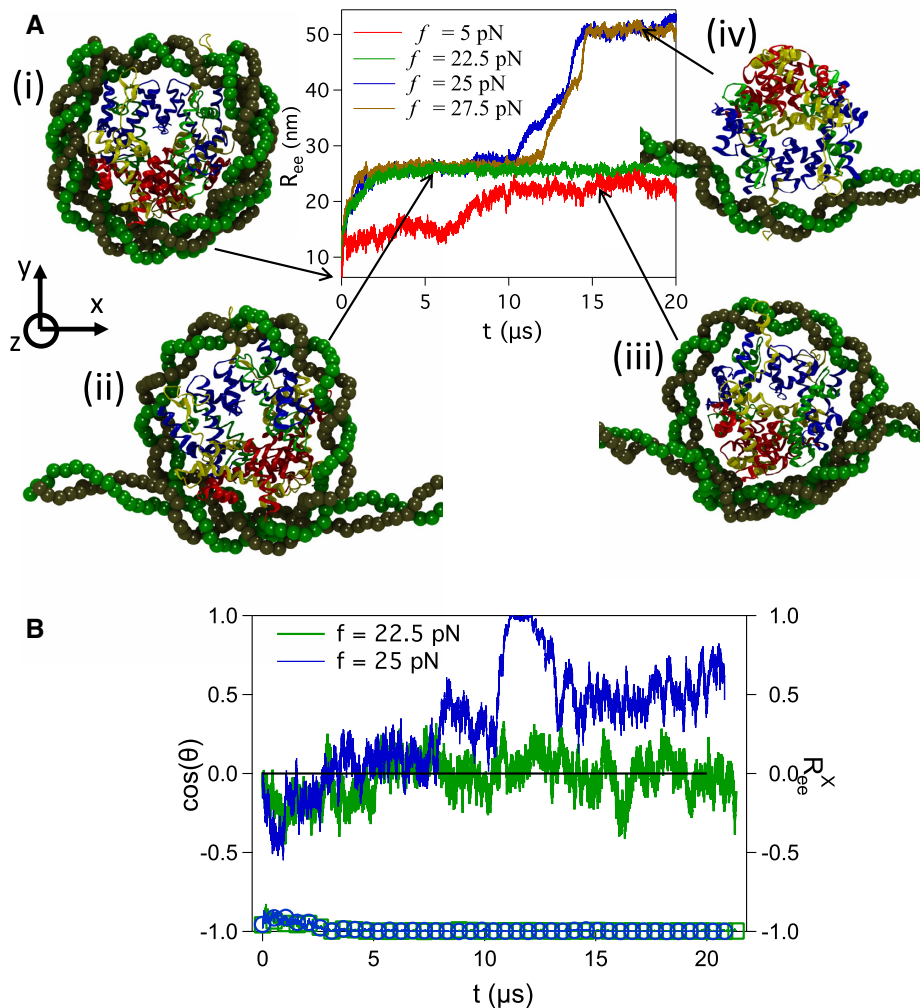
Figure 2. (**A**) Stages in DNA unwrapping when the force ($\vec{f}$) is applied along the *x* direction. In the initial conformation, the dyad axis of the nucleosome ($\vec{D}$), principal moment of inertia of the HPC ($\vec{I}$), and DNA end-to-end distance ($\vec{R}_{ee}$) point along the *y, z* and *x* directions, respectively. R_{ee} is plotted as a function of time (*t*) at different values of the constant *f*. The sequence of structural changes of the nucleosome that occur in two stages are shown in (i) to (iv). (**B**) The 1.0N state is observed at the end of the transition for $f = 5$ pN (red curve in (A)) at $t \approx 20$ μs and at $t \approx 5$ μs for $f = 22.5$ pN (green curve in (A)). The value of cos(θ) fluctuates around 0 (green), since θ ≈ 90°. At $f = 25$ pN, DNA unwraps completely from the HPC resulting in the transition from 1.0N to 0.5N state (blue curve in (A)), which requires a 180° rotation by the HPC. This rotation is observed between 10 and 15 μs (see the jump in cos(θ)). For both $f = 22.5$ pN (blue circles) and 25 pN (green squares), the *x*-component of the unit of vector of R_{ee}, R_{ee}^X is ≈ -1, indicating that R_{ee} is along the *x* direction and does not change orientation during the transitions.

the first stage (Figure 2A(i) to A(ii)/(iii)). Our simulations show that the peeling of the outer wrap occurs at a force of ≈5 pN (see the time dependent changes in $R_{ee}(t)$ in Figure 2). During this transition the extension of the DNA, R_{ee}, increases by ≈21–22 nm, with the experimental value being ~21 nm. Although simulations capture the length increase in DNA as well as the forces at which the first unwrapping transition occurs fairly accurately, the simulations cannot account for the hopping transitions (between the wrapped and unwrapped states) observed in experiments (12,14). The time scale for hopping transitions are on the order of a second whereas, even using coarse-grained simulations, one can only reach times on the order of tens of μ*s*.

The second rip, which occurs when *f* exceeds ≈10 pN, involves a transition to the 0.5N state from the 1.0N state

(Figure 2A(ii) to A(iv)). The increase in extension in the second transition is ≈25 nm, which is also in agreement with 22 nm measured in experiments. In our simulations, only when *f* exceeds 25 pN there is an irreversible 1.0N → 0.5N transition on the time scale of simulations (tens of μsecs) (Figure 2A(ii) to A(iv)). DNA unwrapping transitions are found to be similar in multiple simulation trajectories (Supplementary Figure S1).

The findings in the simulations are in reasonable accord with experiments. In the pulling experiments (12), the first transition is centered at ≈3 pN and whereas the second rupture has a most probable value of ≈9 pN. However, the distribution of measured rupture forces is broad. In our simulations, the corresponding forces are ≈5 pN and ≈25 pN, respectively. It is worth noting that forces in the range of ≈15–30 pN might be required to unwrap the inner turn (12,14)

depending on the loading rate. Considering that we did not choose the model parameters to reproduce any feature of the pulling experiments, we surmise that the SOP simulations semi-quantitatively reproduce the two stage DNA unwrapping found in experiments.

The larger average rupture forces, compared to experiments, for the second transition is due to the limitations on the length of the simulations. The traces are on a time scale of seconds in the experiments, whereas the maximum time scale achievable, even using the coarse-grained SOP model, is only on the order of tens of microseconds. Therefore, it is necessary to use high forces (by implication high pulling speeds) in order to observe the unwrapping events in about 10–20 μs. The most probable unbinding force for the second non-equilibrium transition (see below) is expected to scale as ln (v) (42), where v is the velocity with which one end of the protein is pulled keeping the other end fixed. Therefore, we believe that the unwrapping mechanism would not change significantly even if the mean rupture force for the second transition in the simulations is larger than in the experiments.

Forced unwrapping induces HPC rotation

Pulling experiments and computational studies have largely focused on the forced-unwrapping of the DNA. How the HPC responds to the forces applied to DNA is unknown. It is clear from the KS model (22), and the early studies by Cui and Bustamante (6) that HPC must rotate during the rupture of the inner turn, although the details of how this transpires cannot be elucidated using the cylinder representation of the HPC or from experiments. We find that during the $1.0\mathbf{N} \rightarrow 0.5\mathbf{N}$ transition, the HPC undergoes a 180° rotation in agreement with the previous studies (6,22). As the HPC rotates, the direction of the principal moment of inertial vector associated with the HPC, $\vec{I}$, which initially points in the z direction, undergoes 180° rotation in the xz-plane around the y direction. In contrast, $\vec{R}_{ee}$, which was along the x direction does not undergo any change in orientation.

The HPC rotation is quantified using $\cos(\theta)$, where θ is the angle between the vectors $\vec{I}$ and $\vec{R}_{ee}$ (see equations (S3) and (S4) in the SI for details). The angle θ varies from either −90° to 90° or 90° to −90° during the 180° rotation of the HPC in the xz-plane (Figure 2B). The abrupt jump in $\cos(\theta)$ (from ≈0 to ≈+1 in Figure 2B) is evidence of HPC rotation, occurring on a time scale ≈ (20–30)μs, during the unwrapping of the inner turn. In contrast, the x-component of the end-to-end unit vector, R_{ee}^{X}, is pinned at ≈−1 during the HPC rotation indicating that the direction of $\vec{R}_{ee}$ does not change during the $1.0\mathbf{N} \rightarrow 0.5\mathbf{N}$ transition (Figure 2B). The torque required for the rotation of the HPC increases the (kinetic) barrier for the unwrapping of the inner turn (see below for a rough estimate).

Outer turn unwrapping transition is reversible

In order to demonstrate that the peeling of the inner wrap of the DNA is reversible, we applied $\vec{f}$ along the z direction (perpendicular to $\vec{R}_{ee}$) on one end of the DNA while keeping the other end fixed. The stretching energy is $\vec{f} \cdot \vec{R}_{ee}$ with

$\vec{f} = (0, 0, f)$. The nucleosome was aligned in the same orientation as before ($\vec{R}_{ee}$, $\vec{D}$ and $\vec{I}$ approximately point along the x, y and z directions, respectively) (Figure 3A(i)). In this geometry, $\vec{f}$, which is perpendicular to $\vec{R}_{ee}$ does not propagate along the contour of the DNA. As before the $1.6\mathbf{N} \rightarrow 1.0\mathbf{N}$ transition occurs at $f \approx 5$ pN. The time dependent changes in $R_{ee}(t)$ in both the pulling geometries are almost identical (compare the red curves in Figures 2 and 3). The independence of the unwrapping of the outer turn on the pulling geometry suggests that this transition is reversible.

The $1.0\mathbf{N}$ state is observed for f in the range 5 pN $\leq f \leq$ 20 pN (Figure 4). During the $1.6\mathbf{N} \rightarrow 1.0\mathbf{N}$ transition, the whole nucleosome rotates by 90° in the xz plane about the y direction as the applied force realigns $\vec{R}_{ee}$ along the force direction (z direction) (Figure 3A(i) to A(ii) and B). Upon rotation, the vectors $\vec{R}_{ee}$, $\vec{D}$ and $\vec{I}$ of the nucleosome point along the z, y and x directions, respectively (Figure 3A(ii)). As a consequence, R_{ee}^{X} decreases from ≈1 to ≈0 in ≈ 2.0 μs after the application of force (Figure 3B). We do not detect the 90° rotation of the nucleosome from the plots of $\cos(\theta)$ as both $\vec{R}_{ee}$ and $\vec{I}$ simultaneously undergo 90° rotation around the y direction (Figure 3C).

Population of the 1.0N state depends on both the magnitude of force and the pulling direction

We next performed simulations at $f = 20$ pN applied along the z direction. The time dependence of $R_{ee}(t)$ (the green line in figure 3A) shows the familiar two stage unwrapping transition. The lifetime of the $1.0\mathbf{N}$ state is at least ≈ 10 μs (Figure 3). Such a long lifetime suggests that for the $1.0\mathbf{N} \rightarrow 0.5\mathbf{N}$ transition there must be a free energy barrier because the HPC must rotate by 180°, as shown earlier (see Figure2B) when the force was applied along the x direction (Figure 3C). During the HPC rotation, only the moment of inertia $\vec{I}$ rotates by 180°, while $\vec{R}_{ee}$, which points along the z direction does not change orientation even during the inner unwrapping transition.

In contrast, when $f = 25$ pN is applied perpendicular to $\vec{R}_{ee}$, the $1.0\mathbf{N}$ state is not detected in the transition to the $0.5\mathbf{N}$ state (see the blue line in Figure 3). Comparison of the structures, Figure 3A(ii) and A(iii), shows dramatic differences. At this force, $\vec{R}_{ee}$ become parallel to $\vec{f}$ in the initial ≈2 μs (Figure 3B). In this short time, >1.0 turn of DNA is unwrapped. As a consequence, the $1.0\mathbf{N}$ state is not populated in this pathway (Figure 3A(iii)). We find that at very large forces there is a continuous transition from the $1.6\mathbf{N}$ to $0.5\mathbf{N}$ state bypassing the $1.0\mathbf{N}$ state (Figure 3A(iii), B, C). We find similar DNA unwrapping transitions from the HPC in several independent simulation trajectories (Supplementary Figure S2).

Role of histone tails

To ensure that the two-stage unwrapping mechanism is robust, we performed simulations to assess the role of histone tails (see SI for details). We find that the unwrapping mechanisms are similar with and without histone tails. However, due to additional favorable interactions between the histone
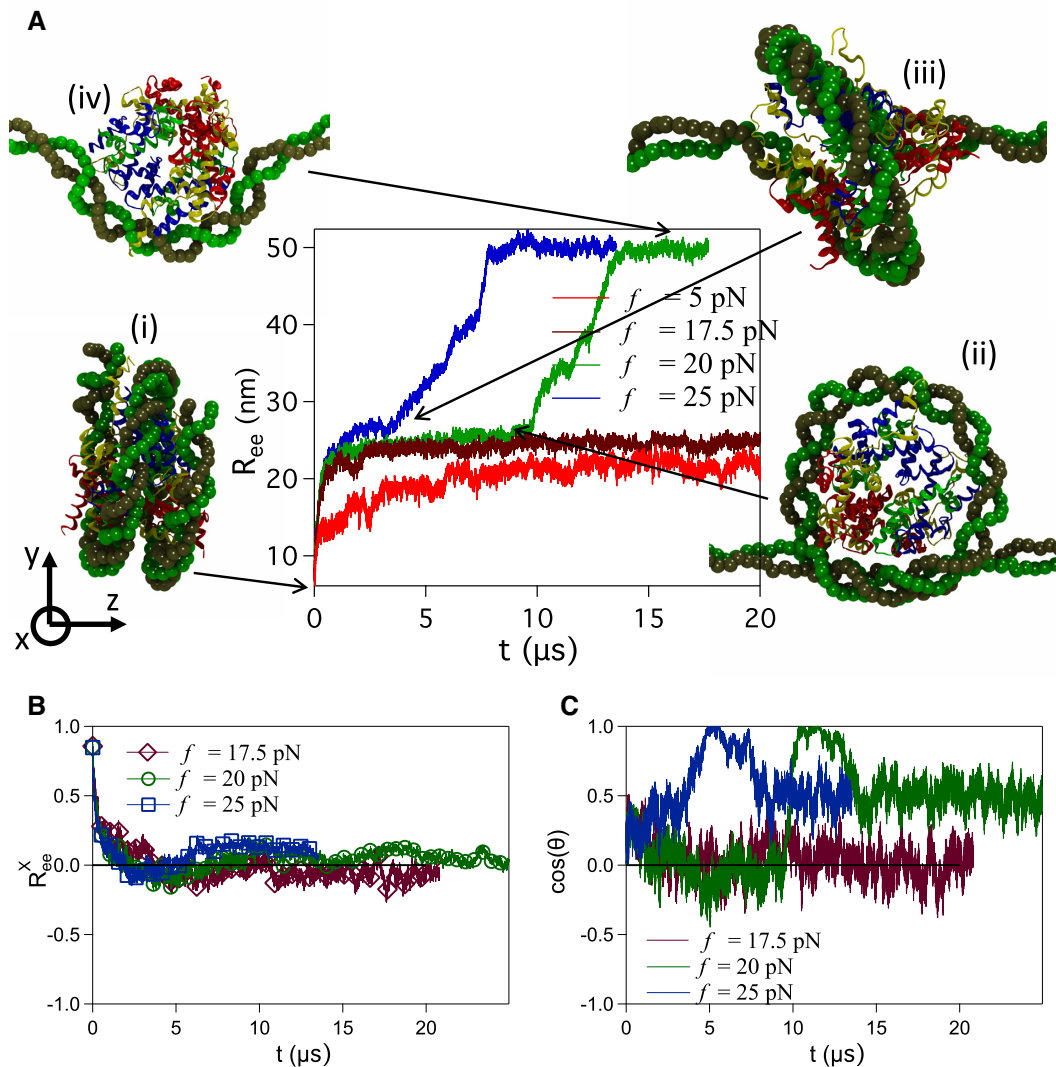
Figure 3. Pulling DNA along the z-direction. (**A**) At $t = 0$, $\vec{D}$, $\vec{I}$ and $\vec{R}_{ee}$ are along the y, z and x directions, respectively. R_{ee} is plotted as a function of t. (**B**) In the initial 2 μs, as $\vec{R}_{ee}$ aligns along $\vec{f}$, the direction R_{ee}^X decays to ≈ 0. (**C**) At $f = 17.5$ pN, 1.0N state is observed at the end of the first transition. On this time scale $\cos(\theta)$ fluctuates around 0. At $f = 20$ pN, DNA unwraps completely from the HPC. The transition from 1.0N to 0.5N state, which requires a 180° rotation by the HPC occurs between 10 and 15 μs ($\cos(\theta)$ jumps abruptly in the green trajectory). At $f = 25$ pN, DNA continuously unwraps from the HPC as it rotates with the jump in $\cos(\theta)$ occurring on shorter times.

tails and the DNA, the magnitudes of the rupture forces, especially for the second transition (1.0N → 0.5N), are higher. The average extensions in R_{ee} at the end of the transitions, as a function of the applied f along the x direction ($\vec{f}$ parallel to $\vec{R}_{ee}$) and z direction ($\vec{f}$ perpendicular to $\vec{R}_{ee}$) are shown in Figure 4. An external force between 5 and 8 pN is required to observe the first transition irrespective of the direction of the applied force. The dependencies of R_{ee} on f are similar at forces at which outer unwrapping is observed, resulting in the population of the 1.0N state.

In the presence of histone tails, a higher value of force is required to observe the 1.0N → 0.5N transition. Because the tails are present on either side of the DNA (see Figure 1A), resulting in favorable electrostatic interactions with the DNA, the magnitude of force needed for unwrapping increases. As a result, the 180° rotation of the HPC, required

for the second transition, is further hindered as the applied force has to overcome the favorable electrostatic interactions between the DNA and histone tails, in addition to the solvent induced frictional forces that prevent the HPC rotation. It is reassuring that the range of unwrapping forces, even in the presence of histone tails, is in agreement with experimental estimates. Apart from the differences in the rupture forces the nature of the two stage transition is not qualitatively affected.

Differences in wrapping and unwrapping mechanisms explain hysteresis

In order to determine the differences in the assembly (rewrapping from the stretched 0.5N state to the 1.6N state) and forced-unwrapping of DNA, we performed force

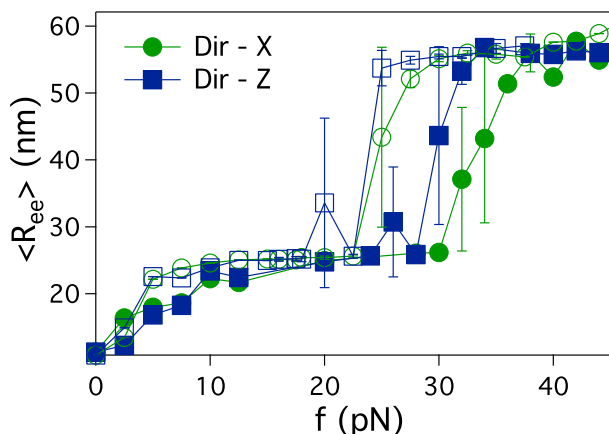**Figure 4.** Average R_{ee}, $\langle R_{ee} \rangle$ plotted as a function of f. The open (closed) symbols represent results without (with) histone tails. The superposition of all the curves at low forces once again shows that the unwrapping of the outer turn is reversible. The charged residues in the histone tails interact with the DNA and prevent the rotation of the HPC. DNA unwraps from the HPC at higher forces compared to when the histone tails are absent. Inclusion of the histone tails does not alter the global unwrapping mechanism. For each data point, the DNA is pulled at constant f for at least 6×10^8 Brownian dynamics simulation time steps, which is ≈ 15 μs.

quench simulations. The nucleosome is first prepared in the 0.5**N** state by applying a constant force, and subsequently the force is quenched to $f_Q = 0$ (may be difficult to realize in experiments). Note that the direction of pulling does not affect the formation of the fully unwrapped (0.5**N**) state. If the transitions were reversible, we would expect the assembly pathway 0.5**N** $\leftrightarrow$ 1.0 **N** $\leftrightarrow$ 1.6**N**. Instead, we find that rewrapping mechanism upon force quench to $f_Q = 0$ pN (Figure 5) is dramatically different from the force-induced unwrapping pathway (Figure 2). When $f_Q = 0$, the HPC rotation does not occur because in the DNA ends are unrestricted in the simulations. As a result, DNA undergoes stochastic fluctuations as it rewraps around the HPC (Supplementary Figure S3). The two free ends of the DNA slide past one another in order to wrap around the HPC (Figure 5(iii) and (iv)). However, this wrapping pathway is prohibited in single molecule pulling experiments as the ends of the DNA are pinned by attaching them through a handle to a polystyrene bead held in an optical trap (12). Hence, the DNA ends cannot readily wrap around the HPC.

The situation in the optical trap experiments can be mimicked in the simulations if $f_Q \neq 0$. In such a setup, DNA can rewrap around the HPC only when $\vec{I}$ of the HPC aligns with the direction of $\vec{f}$ (x direction) (see Figure 6(iii)). The time dependent decrease in $R_{ee}(t)$ in the representative rewrapping trajectory for $f_Q = 3$ pN shows that upon force quench, $R_{ee}(t)$ decreases by ≈ 15 nm (the green curve in Figure 6) rapidly. The structures that are sampled during the long time period when there is a plateau in both $R_{ee}(t)$ and $\cos(\theta)$ correspond to the 0.5**N** state. The time dependent changes in $R_{ee}(t)$ further shows that 0.5**N** $\rightarrow$ 1.0**N** transition, which takes place between 30 and 40 μs is the key event in the assembly process. It should be pointed out that at $t \approx 30-40$ μs the value of R_{ee} is similar (the green curve in Figure 6) to that found after outer turn forced unwrapping (see

Figure 2), implying that the 1.0**N** state is sampled during unwrapping and rewrapping processes. The formation of the 1.0**N** state both during unwrapping and upon force quench affirms that the first transition is reversible. The 1.0**N** $\rightarrow$ 1.6**N** transition leading to the complete rewrapping of the DNA on the HPC occurs rapidly when the jump in $\cos(\theta)$ is complete.

Note that prior to the 1.0**N** $\rightarrow$ 1.6**N** transition, $\cos(\theta)$ jumps to unity (red curve in Figure 6) before decreasing to zero when the nucleosome with the fully wrapped DNA reforms. Naively, it may appear that the spike in $\cos(\theta)$ is the reverse of event that occurs when unwrapped at high forces (see the blue curve in Figure 2B). However, in the latter case the sudden increase in $\cos(\theta)$ is directed in the sense that the mechanical force generates a torque along a specific direction causing the observed rotation. In sharp contrast, in the reassembly process the alignment of $\vec{I}$ of the HPC along the direction of $\vec{f}$ occurs stochastically due to thermal fluctuations of the HPC (Figure 6(iii)). In this orientation, the arms of the DNA leaving the HPC smoothly bend in the direction of $\vec{f}$ (Supplementary Figure S4). Thus, in the process of rewrapping of the DNA on HPC, force does not play any role in aligning $\vec{I}$ of the HPC along the $\vec{f}$ direction. The applied 3 pN force does not generate torque in the direction opposite to what was observed during DNA unwrapping by force. Alignment of HPC in a favorable orientation for DNA wrapping is a random event. The different role f plays in the wrapping and unwrapping pathways of the DNA contributes to the observed hysteresis in the force–extension curve for the nucleosome (12). Thus, inherently the kinetically driven second unwrapping transition exhibits non-equilibrium signatures. Similar DNA wrapping mechanism is also observed for force quenches to $f_Q = 2$ and 4 pN (Supplementary Figure S5) and in multiple independent trajectories generated at lower forces (Supplementary Figure S6).

Rotational barrier in the unwrapping of the inner turn

In order to fully unwrap the DNA from the populated 1.0**N** state, the magnitude of f must be sufficiently large to generate the needed *torque to rotate* the HPC by 180° in water. In order to account for histone rotation, we modified the KS (22) theory, which models DNA as a wormlike chain (WLC) of length, L, and stiffness κ. The HPC is modeled as a cylinder with radius, R. The WLC is adsorbed on the cylinder in a helical manner with a pitch, H. The torsional stiffness of the WLC is neglected because the ends of the DNA are free to rotate. As force f is applied to the WLC (Supplementary Figure S7), the WLC bends and desorbs from the cylinder and simultaneously causes the cylinder to rotate. The desorption angle α describes the length of the WLC adsorbed on the cylinder ($\alpha = 0$ and π correspond to the 1.0**N** state, and nearly completely unwrapped state, respectively). The angle β, accounting for the degree of rotation of the cylinder, describes the orientation between the axis of the cylinder, $\hat{n}$, and the z direction (Supplementary Figure S7). Due to the symmetry in the system, the axis of the cylinder, $\hat{n}$, rotates only in the yz plane. The total energy of the mechanical representation of the nucleosome is,

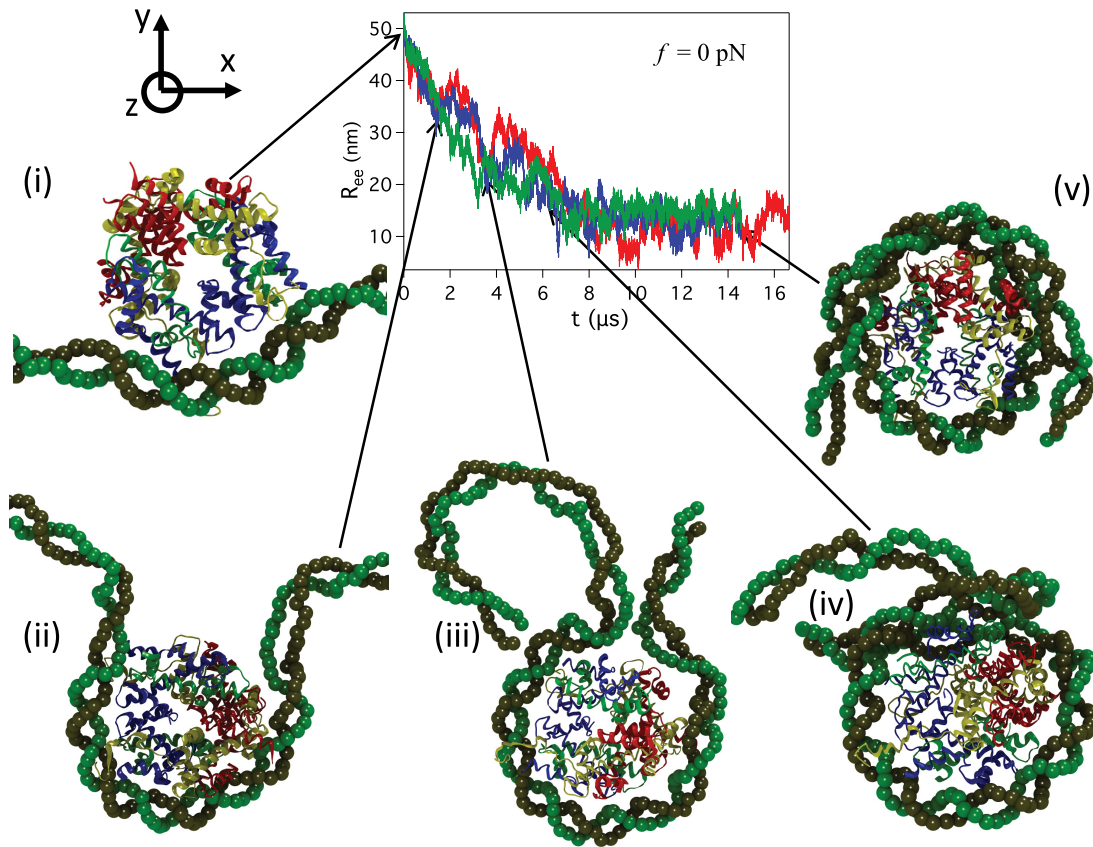$$E_R(\alpha, \beta) = E_{NR}(\alpha, \beta) + E_{rot}(\alpha, \beta), \qquad (1)$$

Figure 5. Rewrapping of DNA around the HPC upon force quench. Displayed are the structural transitions at select time points in the pathway to form a fully wrapped nucleosome after quenching the force to $f_Q = 0$ pN. The time-dependent decrease in R_{ee} in the three different trajectories, shown in red, blue and green, are superimposable.
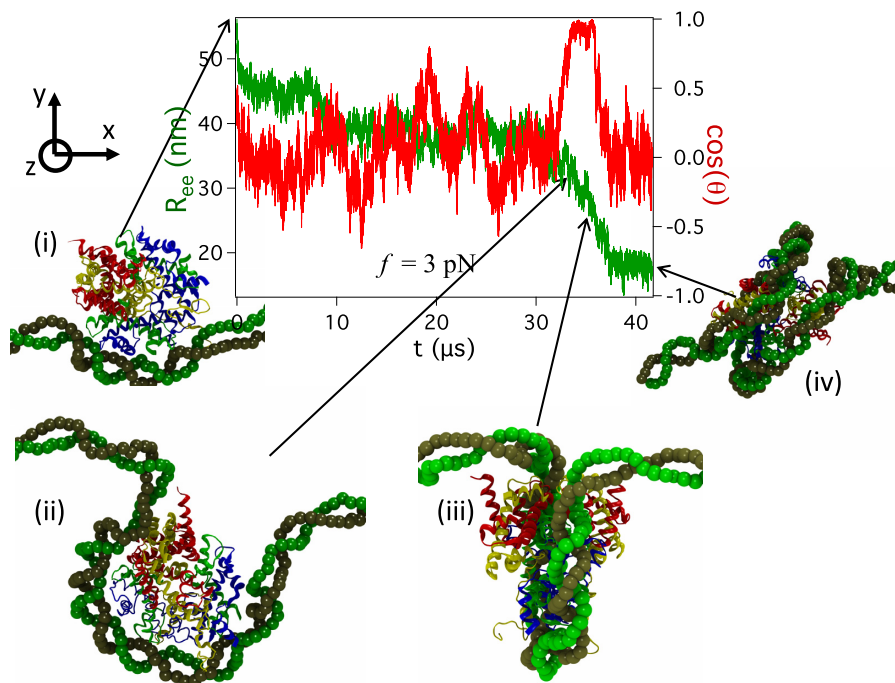

Figure 6. Rewrapping dynamics. R_{ee} and $\cos(\theta)$ are plotted as a function of t for a DNA folding trajectory for $f_Q = 3$ pN.

where $E_{NR}(\alpha, \beta)$ (22) is reproduced in the SI.

Estimation of E_{rot}

We calculated the contribution of the barrier to HPC rotation, E_{rot}, using the elastic model. The energy required to rotate the cylinder through an angle β by the torque, $\tau(\alpha, \beta')$, generated due to f acting on the WLC arms is,

$$E_{rot}(\alpha, \beta) = - \int_0^\beta \tau(\alpha, \beta') \, d\beta'. \qquad (2)$$

The generated torque increases the transition energy barrier for the nucleosome to go from the 1.0**N** state ($\alpha = 0$) to the state where DNA is completely unwrapped ($\alpha = \pi$).

Plots of $\tau(\alpha, \beta)$ (equation S13) and $E_{rot}(\alpha, \beta)$ (equation S14), calculated numerically as a function of α, subject to the constraint (equation S8) for different f are shown in Supplementary Figure S8 (details in the SI). The addition of $E_{rot}(\alpha, \beta)$ to the energy of the WLC and cylinder system increases the transition barrier to fully unwrap the DNA (Figure 7A). For $f = 0.8 \, k_B T/\text{nm}$, the barrier for WLC unwrapping from the cylinder increases by $\approx 2.5 \, k_B T$ due to $E_{rot}(\alpha, \beta)$ (Figure 7A). The energy difference between the DNA wrapped state and unwrapped state, $\Delta E_R (= E_R(\alpha \approx \pi) - E_R(\alpha \approx 0))$ and $\Delta E_{NR}(= E_{NR}(\alpha \approx \pi) - E_{NR}(\alpha \approx 0))$, as a function of f shows that the requirement to rotate the cylinder increases the transition barrier, and the energy difference between the states $\alpha \approx \pi$ and $\alpha \approx 0$ for all f. Thus, a larger f than previously estimated would be needed to unwrap the DNA from the cylinder (Figure 7B).

It is important to note that the calculated increase in the barrier using equation (2) is a lower bound. In addition to the purely energetic barrier arising from the elastic model there is a penalty ($E_{dyn} \propto \eta R H$, where η is the viscosity of water) to rotate the cylinder through the viscous medium. The resulting kinetic barrier would further enhance the total barrier that must be surmounted to unwrap the outer turn.

DISCUSSION

We used constant force simulations using the coarse-grained SOP model, without any adjustable parameter, to determine the structural transitions that take place during unwrapping of human α-satellite DNA sequence from the nucleosome as well as in the assembly process upon quenching the force. Our simulations, using a single bead resolution of the 1268 combined number of nucleotides and residues of histone proteins, is consistent with the two stage unwrapping transition observed in several experiments. The length of DNA released in the two transitions are in excellent agreement with single molecule pulling experiments (12). The global two stage transition is found to be nearly independent of DNA sequence (experiments and simulations often use the Widom high affinity nucleosome 601 sequence), implying that certain aspects of unwrapping depends only on the nucleosome structure. This is similar to the finding that native topology determines the force induced unfolding pathways of globular proteins (43).
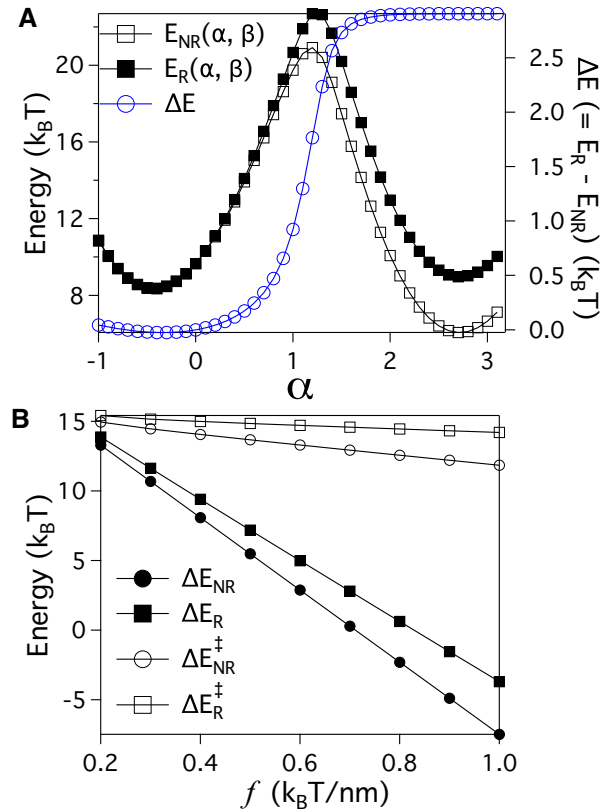

Figure 7. (**A**) Plot of $E_R(\alpha, \beta)$ (solid squares), $E_{NR}(\alpha, \beta)$ (empty squares) and $\Delta E (= E_R(\alpha, \beta) - E_{NR}(\alpha, \beta))$ (blue empty circles) as a function of α. Due to the HPC rotation, the barrier for DNA unwrapping increases by $\approx 2.5 \, k_B T$. (**B**) $\Delta E_R (= E_R(\alpha \approx \pi) - E_R(\alpha \approx 0))$ (solid squares) and $\Delta E_{NR}(= E_{NR}(\alpha \approx \pi) - E_{NR}(\alpha \approx 0))$ (solid circles) as a function of f. $\Delta E_R^\ddagger (= E_R^{max} - E_R(\alpha \approx 0))$ (empty squares) and $\Delta_{NR} E^\ddagger (= E_{NR}^{max} - E_{NR}(\alpha \approx 0))$ (empty circles) as a function of f. Here, E_R^{max} and E_{NR}^{max} is the maximum (corresponds to the transition region) in the energy during the transition from $\alpha \approx 0$ to $\alpha \approx \pi$ state. Note that if the dimensions of the cylinder and the value of α are known, then the HPC rotation angle can be calculated using Eq. (S8) in the SI. The HPC parameters are $R = 4.2$ nm, $H = 2.5$ nm, $l_p = 50$ nm, $\epsilon_{ads} = 0.7 \, k_B T$, and $f = 0.8 \, k_B T/\text{nm}$.

Energetics and time scales of outer turn unwrapping

The critical force, f_{cI}, for the first reversible transition (centered at approximately at ≈ 3 pN or ≤ 6 pN in experiments (12,14) and ≈ 5 pN in our simulations) is needed to overcome the interactions of the outer turn of the DNA with histones. The lack of dependence of the outer turn rip on the pulling direction (Figure 4) confirms that outer loop of the DNA reversibly wraps and unwraps around the HPC. We conclude that the apparent barrier ($\approx 15 \, k_B T$), not that dissimilar to the energy required to unbind the outer turn (22), which we take to be the minimum free energy barrier. Our estimate for the barrier height when combined with the attempt frequency (30) of $k_0 \approx 4.0 \times 10^6$ yields a rupture time for outer turn (as per Kramers theory) on the order of 800 ms at zero force, which is not inconsistent with the results in (14,44,45).

We note that the estimates of outer turn unwrapping time (lifetime of the fully wrapped state) seems to vary widely, ranging from about 250 ms using FRET and time-resolved

SAXS experiments (44,45) to ten seconds or more using pulling experiments (see Figure 4b in (13) for comparison between three data sets). Although experiments using mechanical forces have provided considerable insights into the disassembly of single nucleosomes, it is unclear if extrapolation using $f \neq 0$ measurements to $f = 0$ to extract the lifetimes of the wrapped or unwrapped states is reasonable. More importantly, the validity of using extension as the sole reaction coordinate for a complex DNA-protein complex is unclear. Even for the simpler cases of force-induced unfolding of globular proteins and RNA, extension is often inappropriate (46). Nevertheless, considering the uncertainties in the different experimental techniques and protocols (13,44,45) and the limitations of theory and simulations, it is likely that the time scale for outer unwrapping transition, at zero force, is likely to be between 250 ms to about a second.

Rupture of the inner turn

The second transition in which the inner loop of the DNA unwraps is to a large extent cooperative (see Figure 4), which accords well with pulling experiments using magnetic tweezers (47). This transition, which could have short-lived intermediates at high pulling forces (see $R_{ee}(t)$ plot in Figure 2A), is not reversible (12), thus making it difficult to estimate the stability and free energy barrier to rupture. The mechanical energy needed for this transition is $\approx 75 \, k_B T$, which is substantial. The minimum estimate for this transition from experiments is $\approx 45 \, k_B T$, which is the product of the unbinding force (≈ 9 pN) and length gain (≈ 21 nm). Our simulations show that for the inner turn to unwrap, sufficient torque to rotate the HPC by 180°, is required in order to overcome the DNA-histone interactions. The presence of histone tails on either side of the DNA prevent the rotation of the HPC by 180° (Figure 1D), which should increase the mechanical energy needed to disrupt the DNA-HPC interaction.

The rotational barrier has two contributions. One is energetic, which we could estimate using the KS elastic model (Figure 7). The other is kinematic in origin that arises because of the rotation of the HPC moment of inertia. The kinetic barrier is $\propto \eta\omega$ where ω is the angular velocity. The kinematic consequences affect wrapping and unwrapping in totally different ways, leading the asymmetry in the role of histone rotation in the rupture process.

Forced-unwrapping and force-quench assembly

Our simulations show that there is a fundamental difference in unwrapping and reassembly upon force quench. In forced-unwrapping, the torque needed to rotate the HPC comes from force, which facilitates the HPC rotation in peeling the inner turn. When force is quenched (reduced in the release cycle in optical tweezer experiments), the principal moment of inertia of the HPC has to align along the force direction in order for DNA to wrap around the HPC. In contrast to the 'directed' rotation in the unwrapping process, the rotation in the release cycle occurs stochastically. In other words, the external force does not play any role in aligning the HPC. Simulations show that the folding and

the unfolding pathways of the DNA from the HPC during the second transition are different. The difference in the role played by the external force in DNA unwrapping and rewrapping explains the hysteresis observed in experiments.

Prospects for experiments

The major findings of this work are that the histone core rotates during the unwrapping of the second turn in the presence of force as well during the assembly upon force quench from the fully unwrapped state. It is worth restating that HPC rotation plays an entirely different role in the unwrapping and rewrapping processes. When the inner turn is mechanically forced to unwrap, a large force is needed to rotate the HPC in almost deterministic manner (fluctuations in $R_{ee}(t)$ are suppressed). Two experiments might shed light on our predictions. (i) To observe histone rotation it will be necessary to perform three color FRET experiments by labeling two residues on the protein and one on a base pair in the inner turn. Combined force and multiply labelled FRET could be used to discern HPC rotation. We are unsure if such experiments are feasible. (ii) The theoretical model suggests that that the time for unwrapping of the inner wrap would increase as $\exp(c\eta)$, where c is a constant. Thus, small changes in η are predicted to have a large effect on the rate of unwrapping. Naively, it appears that the frictional effect of rotation may be easier to test in experiments.

CONCLUSION

Our simulations show that forced unwrapping and force quench rewrapping of DNA is coupled to histone rotation, which has not been sufficiently emphasized. It is unclear if the response of nucleosomes to force would differ if lysine at various locations (K9 or K27) in the histones are modified. The SOP model can be used to probe the consequences of such post-translational modifications.

We will be remiss if we did not point out the limitations of the study. (i) We have already stated that the duration of the simulations is much shorter than in experiments. Nevertheless, it is surprising that both the length gains in DNA upon unwrapping and the mean forces for rupture are in reasonable agreement with experiments. (ii) We have not explicitly considered hydrogen bond interactions between the nucleotides because the model ignores the DNA sequence, which plays an important role. It will be important to investigate consequences of the sequence-dependent elasticity of DNA (48) although global features of unwrapping (two stage unwrapping and HPC rotation) are likely to be robust. (iii) Just as in experiments, we did not consider the effects of DNA sequence. It is reasonable that the major conclusion that histone rotation must play an important role in the unwrapping dynamics of DNA from the nucleosome would not depend on the sequence. However, because DNA mechanics depends on the sequence (49) it is likely that the magnitude of rotation-induced kinetic barrier as well electrostatic interactions will depend on the sequence. This has to be considered in the future to fully understand the energetics and dynamics of nucleosomes.

SUPPLEMENTARY DATA

Supplementary Data are available at NAR Online.

ACKNOWLEDGEMENTS

FUNDING

REFERENCES

1. Kornberg,R. (1974) Chromatin structure - repeating unit of histones and DNA. *Science*, **184**, 868–871.
2. Andrews,A.J. and Luger,K. (2011) Nucleosome structure(s) and stability: variations on a theme. *Annu. Rev. Biophys.*, **40**, 99–117.
3. Fierz,B. and Poirier,M.G. (2019) Biophysics of chromatin dynamics. *Annu. Rev. Biophys.*, **48**, 321–345.
4. Kornberg,R. and Lorch,Y. (2020) Primary role of the nucleosome. *Mol. Cell.*, **79**, 371–375.
5. Brower-Toland,B., Simth,C., Yeh,R., Lis,J., Peterson,C. and Wang,M. (2002) Mechanical disruption of individual nucleosomes reveals a reversible multistage release of DNA. *Proc. Natl. Acad. Sci. U.S.A.*, **99**, 1960.
6. Cui,Y. and Bustamante,C. (2000) Pulling a single chromatin fiber reveals the forces that maintain its higher-order structure. *Proc. Natl. Acad. Sci. U.S.A.*, **97**, 127.
7. Gemmen,G., Sim,R., Haushalter,K., Ke,P., Kadonaga,J. and Smith,D. (2005) Forced unraveling of nucleosomes assembled on heterogeneous DNA using core histones, NAP-1, and ACF. *J. Mol. Biol.*, **351**, 89.
8. Bennink,M., Leuba,S., Leno,G., Zlatanova,J., de Grooth,B. and Greve,J. (2001) Unfolding individual nucleosomes by stretching single chromatin fibers with optical tweezers. *Nature Struct. Biol.*, **8**, 606.
9. Pope,L., Bennink,M., van Leijenhorst Groener,K., Nikova,D., Greve,J. and Marko,J. (2005) Single chromatin fiber stretching reveals physically distinct populations of disassembly events. *Biophys. J.*, **88**, 3572.
10. Claudet,C., Angelov,D., Bouvet,P., Dimitrov,S. and Bednar,J. (2005) Histone octamer instability under single molecule experiment conditions. *J. Biol. Chem.*, **280**, 19958.
11. Kaczmarczyk,A., Meng,H., Ordu,O., van Noort,J. and Dekker,N.H. (2020) Chromatin fibers stabilize nucleosomes under torsional stress. *Nat. Commun.*, **11**, 126.
12. Mihardja,S., Spakowitz,A., Zhang,Y. and Bustamante,C. (2006) Effect of force on mononucleosomal dynamics. *Proc. Natl. Acad. Sci. U.S.A.*, **103**, 15871.
13. Kruithof,M. and van Noort,J. (2009) Hidden markov analysis of nucleosome unwrapping under force. *Biophys. J.*, **96**, 3708.
14. Ngo,T.T.M., Zhang,Q., Zhou,R., Yodh,J.G. and Ha,T. (2015) Asymmetric unwrapping of nucleosomes under tension directed by DNA local flexibility. *Cell*, **160**, 1135–1144.
15. Hall,M.A., Shundrovsky,A., Bai,L., Fulbright,R.M., Lis,J.T. and Wang,M.D. (2009) High-resolution dynamic mapping of histone-DNA interactions in a nucleosome. *Nat. Struct. Mol. Biol.*, **16**, 124–129.
16. Mack,A.H., Schlingman,D.J., Ilagan,R.P., Regan,L. and Mochrie,S.G.J. (2012) Kinetics and thermodynamics of phenotype: unwinding and rewinding the nucleosome. *J. Mol. Biol.*, **423**, 687–701.
17. Humphrey,W., Dalke,A. and Schulten,K. (1996) VMD - visual molecular dynamics. *J. Molec. Graphics*, **14**, 33.
18. Marko,J. and Siggia,E. (1997) Driving proteins off DNA using applied tension. *Biophys. J.*, **73**, 2173.
19. Kunze,K. and Netz,R. (2002) Complexes of semifleixble polyelectrolytes and charged spheres as models for salt-modulated nucleosomal structures. *Phys. Rev. E*, **66**, 011918.
20. Tsunaka,Y., Kajimura,N., Tate,S. and Morikawa,K. (2005) Alteration of the nucleosomal DNA path in the crystal structure of a human nucleosome core particle. *Nucleic Acids Research*, **33**, 3424.
21. Luger,K., Mader,A., Richmond,R., Sargent,D. and Richmond,T. (1997) Crystal structure of the nucleosome core particle at 2.8 Å resolution. *Nature*, **389**, 251.
22. Kulic,I. and Schiessel,H. (2004) DNA spools under tension. *Phys. Rev. Lett.*, **92**, 228101.
23. Becker,N.B. and Everaers,R. (2009) DNA nanomechanics in the nucleosome. *Structure*, **17**, 579–589.
24. Eslami-Mossallam,B., Schiessel,H. and van Noort,J. (2016) Nucleosome dynamics: sequence matters. *Adv. Colloid Interface Sci.*, **232**, 101–113.
25. Lequieu,J., Schwartz,D.C. and de Pablo,J.J. (2017) In silico evidence for sequence-dependent nucleosome sliding. *Proc. Natl. acad. Sci. U.S.A.*, **114**, E9197–E9205.
26. Sakaue,T. and Lowen,H. (2004) Unwrapping of DNA-protein complexes under external stretching. *Phys. Rev. E*, **70**, 021801.
27. Katritch,V., Bustamante,C. and Olson,W. (2000) Pulling chromatin fibers: computer simulations of direct physical micromanipulations. *J. Mol. Biol.*, **295**, 29.
28. Wocjan,T., Klenin,K. and Langowski,J. (2009) Brownian dynamics simulation of DNA unrolling from the nucleosome. *J. Phys. Chem. B*, **113**, 2639.
29. Ettig,R., Kepper,N., Stehr,R., Wedemann,G. and Rippe,K. (2011) Dissecting DNA-histone interactions in the nucleosome by molecular dynamics simulations of DNA unwrapping. *Biophys. J.*, **101**, 1999–2008.
30. Sudhanshu,B., Mihardja,S., Koslover,E.F., Mehraeen,S., Bustamante,C. and Spakowitz,A.J. (2011) Tension-dependent structural deformation alters single-molecule transition kinetics. *Proc. Natl. Acad. Sci. U.S.A.*, **108**, 1885–1890.
31. Mollazadeh-Beidokhti,L., Mohammad-Rafiee,F. and Schiessel,H. (2012) Nucleosome dynamics between tension-induced states. *Biophys. J.*, **102**, 2235–2240.
32. Zhang,B., Zheng,W., Papoian,G.A. and Wolynes,P.G. (2016) Exploring the free energy landscape of nucleosomes. *J. Am. Chem. Soc.*, **138**, 8126–8133.
33. Lequieu,J., Cordoba,A., Schwartz,D.C. and de Pablo,J.J. (2016) Tension-dependent free energies of nucleosome unwrapping. *ACS Central Sci.*, **2**, 660–666.
34. Parsons,T. and Zhang,B. (2019) Critical role of histone tail entropy in nucleosome unwinding. *J. Chem. Phys.*, **150**, 185103.
35. Hyeon,C., Dima,R. and Thirumalai,D. (2006) Pathways and kinetic barriers in mechanical unfolding and refolding of RNA and proteins. *Structure*, **14**, 1633.
36. Chen,J., Darst,S.A. and Thirumalai,D. (2010) Promoter melting triggered by bacterial RNA polymerase occurs in three steps. *Proc. Natl. Acad. Sci. U.S.A.*, **107**, 12523–12528.
37. Reddy,G., Liu,Z. and Thirumalai,D. (2012) Denaturant-dependent folding of GFP. *Proc. Natl. Acad. Sci. U.S.A.*, **109**, 17832–17838.
38. Denesyuk,N.A. and Thirumalai,D. (2015) How do metal ions direct ribozyme folding?. *Nat. Chem.*, **7**, 793.
39. Mazumder,A. and Kapanidis,A.N. (2019) Recent advances in understanding sigma 70-dependent transcription initiation mechanisms. *J. Mol. Biol.*, **431**, 3947–3959.
40. Chen,J., Chiu,C., Gopalkrishnan,S., Chen,A., Olinares,P., Saecker,R.M., Winkelman,J., Maloney,M.F., Chait,B.T., Ross,W. *et al.* (2020) Stepwise promoter melting by bacterial RNA polymerase. *Mol. Cell.*, **78**, 275–288.
41. Ermak,D. and McCammon,J. (1978) Brownian dynamics with hydrodynamic interactions. *J. Chem. Phys.*, **69**, 1352.
42. Evans,E. and Ritchie,K. (1997) Dynamic strength of molecular adhesion bonds. *Biophys. J.*, **72**, 1541–1555.

43. Klimov,D. and Thirumalai,D. (2000) Native topology determines force-induced unfolding pathways in globular proteins. *Proc. Natl. Acad. Sci. U.S.A.*, **97**, 7254–7259.

44. Li,G., Levitus,M., Bustamante,C. and Widom,J. (2005) Rapid spontaneous accessibility of nucleosomal DNA. *Nat. Struct. Mol. Biol.*, **12**, 46–53.

45. Chen,Y., Tokuda,J.M., Topping,T., Sutton,J.L., Meisburger,S.P., Pabit,S.A., Gloss,L.M. and Pollack,L. (2014) Revealing transient structures of nucleosomes as DNA unwinds. *Nucleic Acids Res.*, **42**, 8767–8776.

46. Morrison,G., Hyeon,C., Hinczewski,M. and Thirumalai,D. (2011) Compaction and tensile forces determine the accuracy of folding landscape parameters from single molecule pulling experiments. *Phys. Rev. Lett.*, **106**, 138102.

47. Sheinin,M.Y., Li,M., Soltani,M., Luger,K. and Wang,M.D. (2013) Torque modulates nucleosome stability and facilitates H2A/H2B dimer loss. *Nat. Commun.*, **4**, 2579.

48. Eslami-Mossallam,B., Schram,R.D., Tompitak,M., van Noort,J. and Schiessel,H. (2016) Multiplexing genetic and nucleosome positioning codes: a computational approach. *PLoS One*, **11**, e0156905.

49. Basu,A., Bobrovnikov,D.G., Qureshi,Z., Kayikcioglu,T., Ngo,T.T.M., Ranjan,A., Eustermann,S., Cieza,B., Morgan,M.T., Hejna,M. *et al.* (2021) Measuring DNA mechanics on the genome scale. *Nature*, **589**, 462467.